Tensile Damage in Quaternary Melamine-Formaldehyde Composites

P.-O. Hagstrand[1], and P. Acuòa[2]

[1] *Department of Polymeric Materials, Chalmers University of Technology*
SE-412 96, Göteborg, Sweden

[2] *Visiting student from University of Oviedo, Spain in the*
Department of Polymeric Materials, Chalmers University of Technology
SE-412 96, Göteborg, Sweden

SUMMARY: A planar random fibre composite (PRFC) based on a recent moulding compound developed by Perstorp AB (Sweden) and DSM (The Netherlands) is studied. The basic material is called Reinforced Melamine Compound (RMC) and consists of a melamine-formaldehyde (MF) matrix filled with alumina trihydrate (ATH) and reinforced with 50 mm long glass fibres. Damage mechanisms are studied in tension by means of *in-situ* scanning electron microscopy. Damage is evaluated by means of stiffness reduction during cyclic straining. The damage rate can be considerably reduced by partly replacing ATH with cellulose for grades where high fire resistance is less important. The main reason this takes place is that due to the strong adhesion, cellulose fibres do not debond from the matrix. ATH particles (mainly larger ones) on the other hand, frequently debond causing stiffness reduction and facilitating crack travel.

KEYWORDS: melamine-formaldehyde, cellulose, cyclic loading, damage, *in-situ* SEM

INTRODUCTION

Planar random fibre composites (PRFC) form an interesting class of composite materials offering several advantages for high volume production. However, these materials are complex and research efforts are needed in order to reach the full potential of these materials. For example, it is well known that, generally, thermoset based PRFCs have a very low design strain value of about 0.2% [1]. In fact, even lower values of around 0.1% can be observed to cause material damage. Perstorp AB (Sweden) and DSM (The Netherlands) are developing a new type of thermoset based PRFC. The material is called Reinforced Melamine Compound (RMC) and consists of a melamine-formaldehyde matrix filled with alumina trihydrate (ATH) and reinforced with 50 mm long glass fibres. The materials are described more in detail in section MATERIALS. In a previous paper [2], tensile damage in different RMC grades reinforced with glass fibre bundles was studied. It was concluded that the presence of fibre bundles cause extensive matrix cracking manifested by a "knee" on the stress-strain curve. Furthermore, it was found that the ATH filler has a negative effect on strength, strain to failure and damage development. Additionally, an RMC grade, belonging to a another RMC type, in which dispersed glass fibres are used as reinforcement, was studied. In that grade very few matrix cracks were formed until failure and as a result, no "knee"

on the stress-strain curve was observed. This is indeed a desirable behaviour if, for example, high surface quality is of interest.

In this work, tensile damage in several grades of this RMC type where further constituents have been added is studied. The main objective is to investigate whether the damage development can be suppressed by changing the resin/filler/fibre composition or replacing the ATH filler with cellulose or calcium carbonate. Damage mechanisms are studied by means of *in-situ* scanning electron microscopy. By mounting a sample in a tensile stage observations of the loaded microstructure can be made with SEM directly during straining. This is a powerful addition to common SEM techniques. *In-situ* SEM has earlier been used for composites [2-6]. Macroscopic damage is quantified from the stiffness reduction measured during cyclic tension by using a damage parameter, *D*. The peak strain is increased in each subsequent loading cycle. Parameter *D* is then correlated with the maximum strain and stress in each cycle. Similar techniques have earlier been used for composites [1, 2, 7-9].

Knowledge and understanding of the damage behaviour is of great importance for further development of the composite. In particular for tailoring the material towards lower propensity to microcracking and higher design strain and strength. The presence of microcracks reduces stiffness, load-bearing capacity and fatigue resistance, as examples. Microcracks may exhibit environmental interaction resulting in degradation. Presence of microcracks causes staining which is particularly undesirable in sanitary applications and similar.

MATERIALS

The main constituents of the moulding compounds are described in the following.

Melamine-Formaldehyde (MF)

Polymers of melamine (2,4,6-triamino-*s*-triazine) and formaldehyde form an important class of amino resins, which have been used commercially for over 60 years. MF is one of the hardest and stiffest isotropic polymeric systems that exist. A flexural modulus as high as 9 GPa has been reported for neat MF [10,11]. It has outstanding scratch resistance and surface gloss. Also advantageous, are temperature resistance, flammability and environmental characteristics. MF is used, for example, in laminates, moulding compounds, coatings and as adhesives. The unique properties of MF make it an interesting case as a matrix for composites.

Glass Mat

All studied grades are reinforced with an E-glass mat in which 50 mm long fibers are randomly distributed. No binder material is used, instead, the fibres are held together mechanically by needling. Here, fibres do not form bundles.

Alumina Trihydrate [12]

Alumina trihydrate (ATH) is a refined mineral filler which is capable of reducing flammability and smoke density of polymers. It is actually not a hydrate, but rather a crystalline aluminum hydroxide, $Al(OH)_3$. It is non-toxic; in fact, amorphous forms of aluminum hydroxide are used in gastric antacid preparations. On heating to temperatures above ~200°C, ATH decomposes endothermically to aluminum oxide and water. The ability to act as a heat sink is the principal reason for its use as a flame retardant in polymers. High filler loading is required to achieve a high fire retarding effect, for example, 40-60 wt.% is often needed. ATH having tensile modulus of 30

GPa and density of 2.42 g/cm^3 generally increases the stiffness and the density of polymers. Like other non-reinforcing fillers it generally lowers the strength and strain to failure, and it carries a slight cost premium over unrefined fillers. The ATH grade used in this study has an average particle size of 6 ìm, given by the manufacturer.

Calcium Carbonate, $CaCO_3$ [13]

Calcium carbonate fillers have high volume usage in plastics mainly due their low cost. They reduce shrinkage during moulding and curing. Furthermore, they are non-toxic, non-irritating and odourless. Another advantage is that they are stable over a wide temperature range, decomposing between 800-900°C. A disadvantage for plastic use is a low resistance to acids. Compared to ATH, calcium carbonate fillers have a slightly lower modulus (26 GPa), and a higher density (2.7 g/cm^3).

Cellulose

Wood consists mainly of cellulose, hemicellulose and lignin. Chemical pulping is the traditional method for separating the cellulose fibres from wood. The physical structure of cellulose fibres consists of several cell walls surrounding a cell cavity in the centre, the lumen [14]. Chemically, cellulose is a linear homopolymer consisting of â-D-glucopyranose units linked together by (1-4)-glycosidic bonds [15]. Cellulose is a semicrystalline polymer. The stiffness of bulk wood is about 10 GPa. Cellulose fibres with moduli up to 40 GPa can be separated by chemical pulping processes. These can be further subdivided into microfibrills with an elastic modulus of 70 GPa [16]. However, a stiffness as high as 134 GPa has been measured for cellulose crystals [14]. Thus, cellulose has an interesting potential as reinforcement. In this study cellulose pulp fibres are used. According to the manufacturer, the average fibre length is 60 ìm and the average thickness is 20 ìm. The cellulose content is 99.5%.

Interactions between MF and Cellulose

MF resins have successfully been used together with cellulose containing materials in a wide variety of applications since many years. For example, MF (and urea-formaldehyde) is widely used as adhesives for plywood and particleboard. MF moulding compounds are most often filled with wood flour, paper pulp, cotton or α-cellulose. A fast growing and an important application for MF resins is hard wearing MF impregnated α-cellulose paper used for preparation of flooring laminates. MF resins are also used as textile finish of cotton fabrics to obtain “non-iron” properties and to enhance wet-strength of paper [17]. Aqueous MF resins can penetrate into cellulose fibres or enter the lumen. This has been confirmed by Hua et al. [18] who used electron spectroscopy for chemical analysis (ESCA) to investigate cellulose fibres treated with a MF resin. Furthermore, MF resins can react with the OH groups in cellulose [19]. The formation of water resistant covalent bonds are regarded to be the reason for the reduction of water sensitivity in MF treated paper and cotton fabrics. Thus, cellulose fibres show strong interactions with MF resins and, consequently, are interesting to analyse as reinforcement.

EXPERIMENTAL

Manufacturing of RMC Laminates

Moulding compounds were manufactured with a pilot impregnation machine at DSM (The Netherlands). The moulding compounds were preheated at 110°C for 45 seconds before they were stacked up in 25 × 25 cm mould, and were compression moulded at 160°C for 120 seconds at a

pressure of 10 MPa to form flat plates of thickness 2.5 to 3.8 mm depending on composition. The condensation water was largely evacuated by venting the mould. The composition of the moulding compounds is shown in Table 1.

Table 1: Composition of studied materials.

Grade	vol % glass	vol % ATH[1]	vol % $CaCO_3$[1]	vol % cellulose[1]
1	15.1	17.2	0.0	8.7
2	15.0	0.0	16.2	8.8
3	19.0	14.3	0.0	11.6
4	15.6	25.2	0.0	0.0

[1] Volume percentage in filled matrix (MF+(ATH or $CaCO_3$) + cellulose + additives.

Measurement of Cyclic Stress-Strain Behaviour

Samples used for cyclic tensile test were of dimensions 25 × 25 mm and were produced by dry cutting from moulded plates with a Buehler Isomet 1000 precision saw equipped with a diamond wafering blade, followed by careful sanding using 400 and 600 paper grades. Samples were conditioned at 21±1 °C and 65±10% relative humidity for at least 24 hours. The cyclic tests were carried out using a Zwick 1455 tensile machine supplied with a clip-on extensometer with a gauge length of 140 mm. Loading and unloading were undertaken at a crosshead speed of 2 mm/min. Damage initiation and evolution were evaluated by conducting cyclic tensile tests in which the maximum strain was increased systematically until failure occurred. In each case the specimens were first loaded to a strain level of 0.05% and then unloaded to zero stress. The maximum strain in subsequent strain-cycles was increased by increments of 0.05%. Between 6 and 11 strain cycles were performed on each specimen. The "damaged" elastic modulus, $E_{D,}$ was found from the central part of the unloading path. The measured values of E_D were then used to define a damage parameter $D = 1 - E_D/E_0$ where E_0 is the "undamaged" unloading modulus (measured on unloading in the 1st cycle). Next, D was correlated with the maximum strain, $\mathring{a}_{mc}$, and stress, $\acute{o}_{mc}$, in each cycle.

***In-Situ* SEM Study of Damage**

For *in-situ* SEM observations, two different kinds of samples were prepared: rectangular shaped for in-thickness direction observations and "dog bone" shaped for in-width direction observations. Samples were manufactured according to the following procedure: 56 × 14.5 mm pieces were carefully cut from grade 1 and 2 plates and machined to obtain the "dog bone" shape. Two 4 mm diameter holes were drilled near the ends. The thickness was reduced to 3 mm by grinding using 400 and 600 paper grades. Finally one of the sides of the samples was polished with 7, 2.5 and 1.25 ìm diamond pastes. The specimens were cleaned in ethanol ultrasound baths between each step of grinding and polishing. Rectangular samples were manufactured similarly: 56 × 14.5 mm pieces were carefully cut from grade 1, 2 and 5 plates. The thickness was reduced to 1.8 mm by grinding with 400 and finally 600 grade sandpaper. The ends were reinforced with 0.5 mm thick steel plates which were glued on with an epoxy adhesive on each side, at both ends. Two 4 mm diameter holes were drilled near the ends of the sample. Finally, one of the longitudinal edges was polished following the same as above procedure. The part of the sample to be studied was sputtered with gold and was mounted in a Raith instrumented heating tensile stage fitted in a Zeiss scanning electron microscope (DSM 940 A). The crosshead speed was set to 2 ìm/s. Instead of using a strain calculated from tensile stage displacement, strains were found at several load levels from observing movement of the free end of a carbon fibre positioned along the sample's

longitudinal axis. The other fibre end was attached to the sample with a small droplet of soft adhesive. The gauge length was set to be equal to the fibre free length plus half of the imbedded length since the fibre at the mid-point of the adhesive droplet is stationary about the sample during straining. Displacement of the carbon free end was measured from SEM with a magnification of 3000 ×, with an estimated accuracy of ±0.7 ìm. Elongation of the sample was stopped few times and damage was observed and recorded.

RESULTS AND DISCUSSION

Cyclic Stress-Strain Behaviour

Stress-strain behaviour of grade 2 subjected to cyclic straining is shown in Fig. 1. For this grade and all other investigated grades hysteretic behaviour is found, indicating the presence of dissipative mechanisms in the materials. After unloading, an apparently irreversible strain is present, this strain increasing with the increasing peak strain in the cycle. At certain strain and stress levels, the unloading modulus starts to continuously decrease until breakage is reached. By measuring the reduction of the unloading modulus, damage development graphs can be constructed.

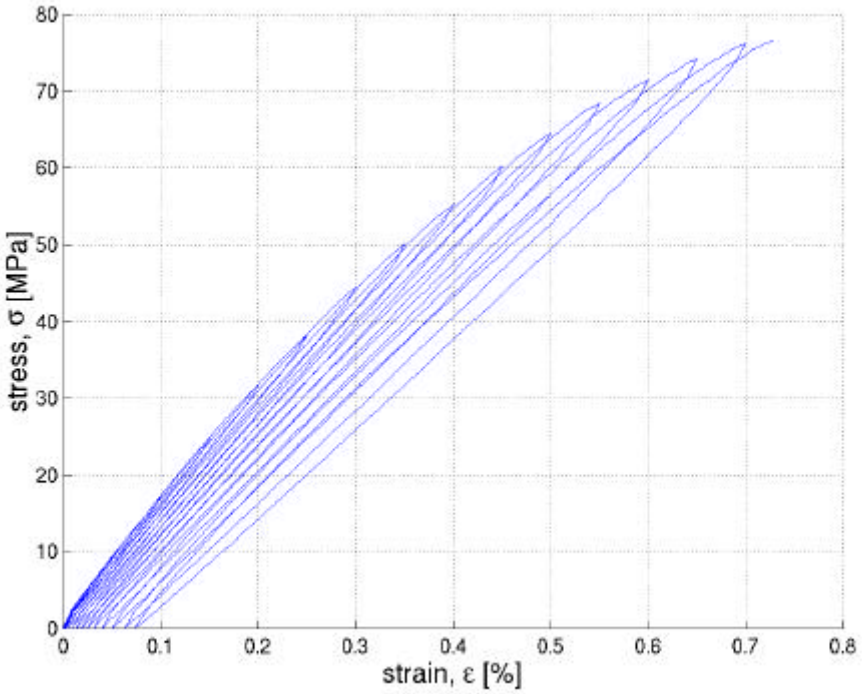

Fig.1: Cyclic stress-strain behaviour of grade 2.

Damage parameter, *D*, is plotted versus maximum cycle strain $\mathring{a}_{mc}$, in Fig. 2. The damage threshold strain, that is the strain below which no measurable damage occurs, appears to be around 0.1% for grades 1, 2 and 4. However, up to 0.15% only very low damage is measured. Grade 3 has a damage threshold strain of 0.25%. Thus, this grade can withstand considerably higher strain levels without being noticeable damaged. The damage rate, d*D*/d$\mathring{a}$, is around 0.66/% for grade 4. Grade 1 and 2 has a damage rate of around 0.33/% below 0.3% strain and around 0.53/% for higher strains. Grade 3 exhibited the lowest damage rate, around 0.43/% above 0.3% strain.

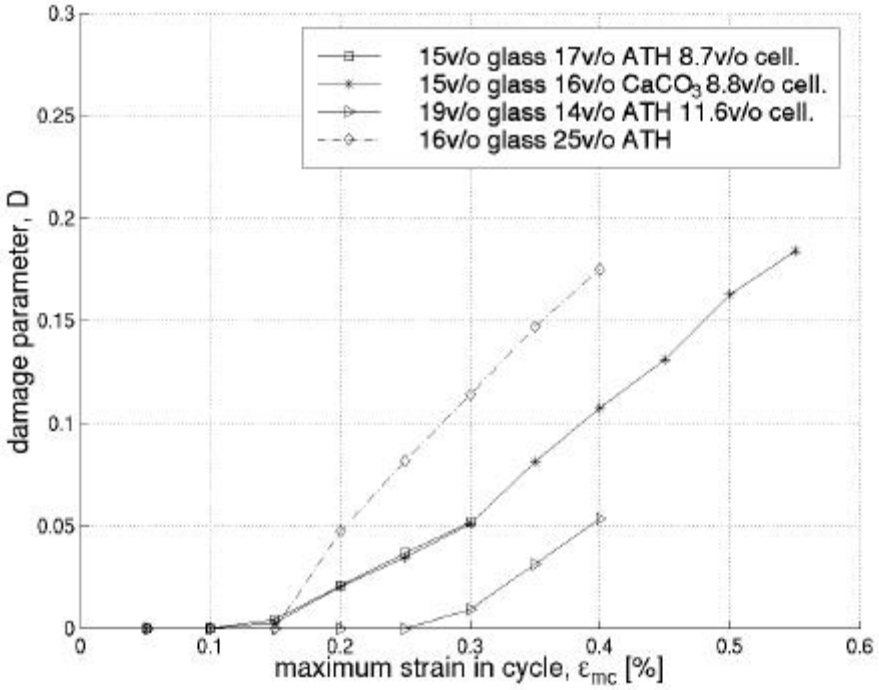

Fig.2: Damage parameter, *D*, versus the maximum strain in cycle, $\mathring{a}_{mc}$.

In Fig. 3, the damage parameter, *D*, is plotted versus the maximum nominal stress in each cycle. The damage threshold stress is around 20 MPa for grades 1 and 2. Grade 4 appears to have a slightly higher damage threshold stress, around 26 MPa. Again, grade 3 exhibits a superior damage resistance with a damage threshold stress around 45 MPa. Similarly to what is seen in Fig. 2, grade 4 has the highest damage rate, d*D*/d*ó* which is approximately $6.6 \cdot 10^{-3}$ /MPa. Other grades, and particularly grade 3, have considerably lower damage rates.

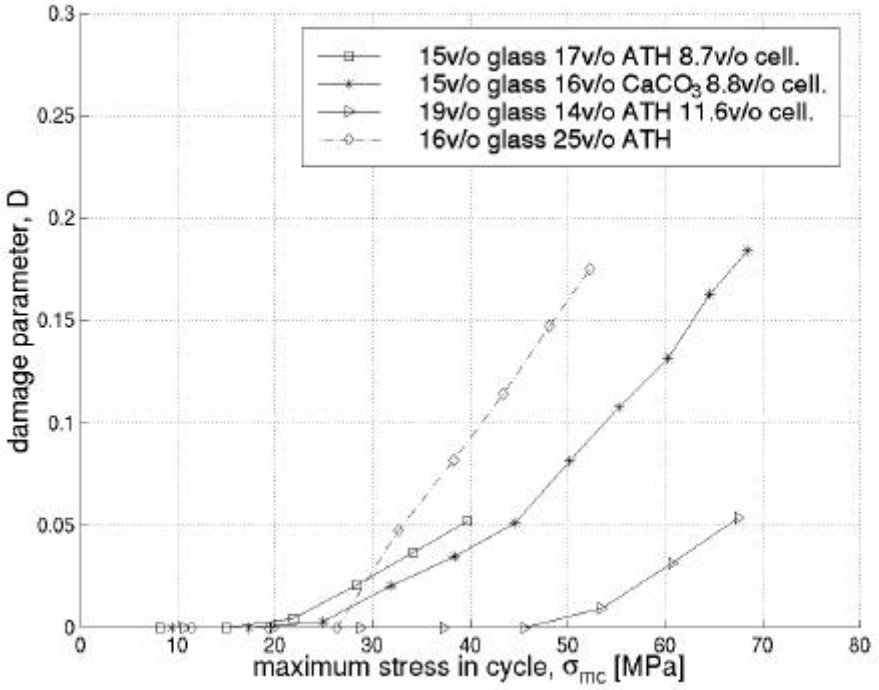

Fig. 3: Damage parameter, *D*, versus the maximum stress in cycle, $\acute{o}_{mc}$.

The influence of constituents on damage behaviour is discussed in the following. As can be seen in Figs. 2 and 3, the damage level caused by loading can be considerably reduced by partly replacing ATH with cellulose. This behaviour can be explained by very high adhesion between cellulose and MF. Also, it can be expected that presence of cellulose generate lower stress concentrations as compared to mineral fillers. ATH particles, mainly larger ones, frequently debond. This contributes to stiffness reduction on loading, and can additionally facilitate crack travel. Cellulose fibres, on the other hand, might act as crack stoppers. Furthermore, the presence of cellulose in MF resins has the potential to lower the void content by absorbing parts of the condensation water. However, cellulose fibres also increase the viscosity of the resin. This makes the impregnation of the glass mat and later, the evacuation of water during venting more difficult. In fact, the lowest void contents were found in grades without cellulose.

Replacing ATH with $CaCO_3$ has no significant measurable effect on damage behaviour. Grade 3 with the highest glass and cellulose content has, as mentioned before, a very low propensity to damage on loading. It is likely that apart from cellulose, the higher glass fibre content also has a positive effect on damage resistance. As mentioned, glass fibres can act as crack initiators. However, as could be observed from SEM micrographs of fractured surfaces, the adhesion between the matrix and the glass is relatively high. Furthermore, the presence of glass reduces the load carried by the matrix. This is possibly the reason for the positive effect of glass fibres on damage behaviour. It is shown elsewhere, that glass fibre bundles on the other hand, are very efficient crack initiators and lower damage resistance [2]. Also, Bourban and co-workers [1] measured lower damage threshold strains and higher damage rates with increasing content of glass fibre bundles.

In-Situ SEM Observations

Before discussing the different damage mechanisms observed during the tensile loading tests, some comments on physical characteristics of ATH, $CaCO_3$ and cellulose, are given. The ATH has a wide size distribution, in fact, particles from 1 to over 50 ìm were observed. As mentioned, the average particle size is 6 ìm according to the manufacturer. ATH particles are relatively irregular. The $CaCO_3$ filler has a more narrow size distribution, the smallest particles being around 1 ìm, and the largest ones less than 10 ìm. The average particle size of the $CaCO_3$ filler is around 4 ìm. In SEM micrographs, the contrast between MF and the imbedded cellulose fibres is very low. This suggests that there is only a small difference in hardness. Possibly, some kind of chemical etching can reveal the cellulose fibres more effectively. The cellulose fibres are sinuous in shape and the average length appears to be around 60 ìm. They are flattened out to a thickness between 5 and 10 ìm from the compression moulding operation.

In-situ SEM samples can be damaged during sample preparation. However, it is possible to distinguish between cracks that have been initiated by sample preparation and these due to straining. The samples are sputtered with gold. Therefore, only cracks caused by straining will be charged by the electron beam. The few pre-existing cracks were inactive and were not observed to propagate on straining.

At a strain of around 0.15%, debonding of glass fibres nearly transversely oriented to the load, and debonding of large ATH and $CaCO_3$ particles was observed. Debonding of fibres was mainly restricted to regions with a relatively high local fibre volume fraction. Cracks were mainly initiated at glass fibres located at free edges and to some extent at debonded glass fibres. The length and the number of cracks increased on further straining. Some cracks were observed to propagate through large ATH particles. No other damage mechanisms were revealed by higher straining.

Micrographs of the fracture surfaces revealed fibres partly covered with matrix. This clearly

suggests that the adhesion between the glass fibres and the matrix is relatively high. For example, in previously studied RMC materials in which a different silane treatment was used, glass fibres in the fracture surface were clean, not covered with matrix [2]. Results from *in-situ* SEM observations show that the adhesion between MF and cellulose is very strong. Debonding of cellulose fibres was never observed, not even at high strain levels. In Fig. 4, cellulose fibres in grade 2 are shown. As mentioned, MF resins can penetrate into the cell wall of cellulose fibres and react with the cellulose molecules [18,19]. This can indeed explain the strong adhesion between MF and cellulose. Also, it is likely that cellulose fibres generate lower stress concentrations in contrast to mineral fillers, as an example. However, a few cracks were initiated in the lumen region, this possibly due to insufficient impregnation of lumen in more central parts of the cellulose fibres. These cracks were never observed to propagate through the cell wall.

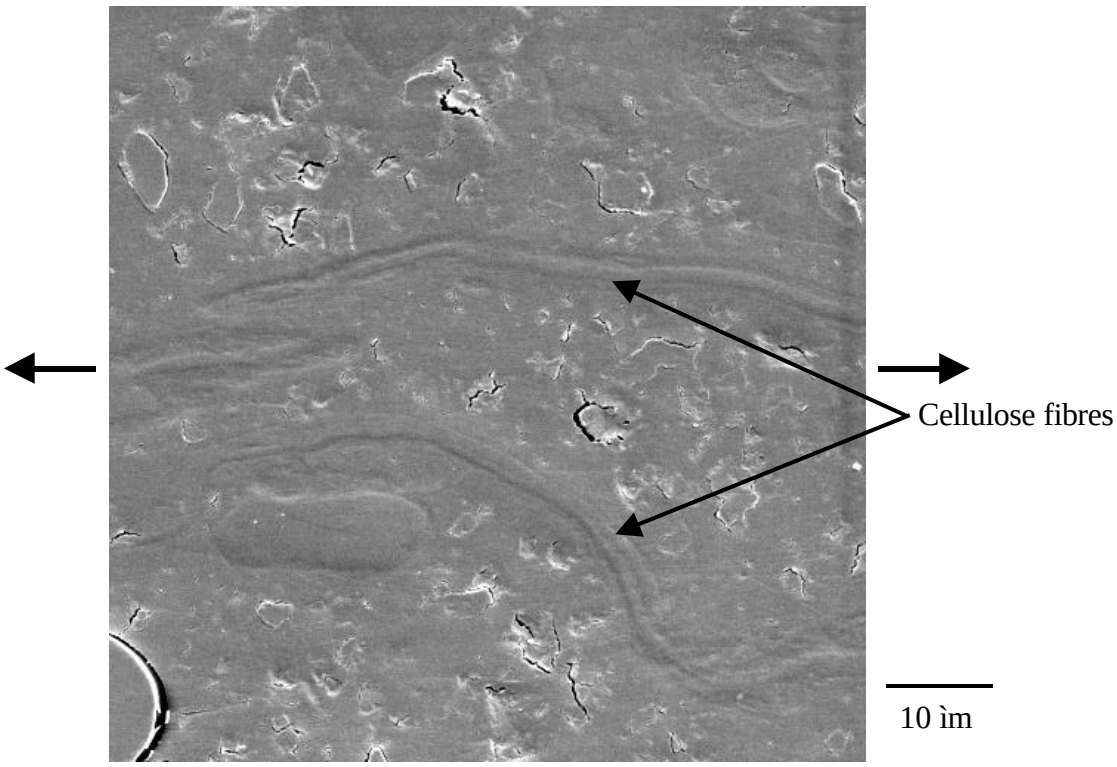

Fig. 4: Cellulose fibres imbedded in calcium carbonate filled MF matrix (grade 2). Loading direction is shown with arrows.

CONCLUSIONS

Tensile damage in various grades of a melamine-formaldehyde composite has been studied. Damage was characterized by means of cyclic loading and was quantified using a damage parameter determined from the reduction of the unloading modulus. It was found that in grades where high fire resistance is less important, damage rate can be considerably reduced by partly replacing ATH with cellulose. Damage mechanisms were studied by means of *in-situ* scanning electron microscopic observations directly under tensile load. Glass fibres, ATH and calcium carbonate particles, debond on loading. This contributes to stiffness reduction, and can additionally facilitate crack. Cellulose fibres, on the other hand, do not debond, and this can be expected from the high affinity of cellulose for MF.

ACKNOWLEDGEMENT

We gratefully acknowledge Perstorp AB (Sweden) for the financial support and DSM Research (The Netherlands) for kindly supplying the materials. The authors are grateful to Dr. S. Lundmark, Mr. H. Persson and Mr. L. Svensson (all Perstorp AB) for valuable discussions.

REFERENCES

1. P. -E. Bourban, W. J. Cantwell, H. H. Kausch and S. J. Youd, *Proc. ICCM9*, Madrid, Spain (1993).
2. P. -O. Hagstrand and R. W. Rychwalski, "Tensile Damage in Ternary M-F Composites", Submitted to *Int. Polym. Processing*.
3. N. Sato, T. Kuranchi, S. Sato and O. Kamigaioto, *J. Mater. Sci*., Vol. 26, 3891, (1991).
4. Y. Q. Sun, J. Tian, J. B. Wang and T. Anderson**,** *Proc. ICCM10*, Whistler, B. C., Canada (1995).
5. A. C. Roulin-Moloney, N. Cudré-Maruroux and H. H. Kausch**,** *Polym. Comp*., Vol. 8, 324, (1987).
6. A. C. Moloney, H. H. Kausch, T. Kaiser and H. R. Beer, *J. Mater. Sci.* Vol.22, 381 (1987).
7. M. C. Yriex, J. Grattier and P. Spiteri, *6èmes Journées Nationales sur les Composites, AMAC*, (1998).
8. D. W. Vogel, Ph. Béguelin, H. H. Kausch and S. J Youd, *Proc. ICCM10*, Whistler, B. C., Canada (1995).
9. M. Steen, C. Filiou and P. Bonnel, *Proc. ECCM8*, Naples, Italy (1998).
10. H. H. Landolt, *Zahlenwerte und Funktionen aus Physik, Chemie, Geophysik und Technik*. Landolt-Börnstein, Berlin (1950).
11. C. Ozinga, DSM Research, Personal Communication, (1995).
12. E. A. Woycheshin and I. Sobolev in *Handbook of Fillers and Reinforcements for Plastics*, H. S Katz and J. V. Milewski, Eds., Van Norstrand Reinhold Company, New York (1978).
13. P. Kummer and G. Crowe in *Handbook of Fillers and Reinforcements for Plastics*, H. S. Katz and J. V. Milewski, Eds., Van Norstrand Reinhold Company, New York (1978).
14. P. Kolseth and A. De Ruvo, in *PAPER Structure and Properties*, J. A. Bristow and P. Kolseth, Eds., Marcel Dekker, New York (1986).
15. R. Ebrahimzadeh, *Ph. D Thesis, Chalmers University of Technology*, Göteborg, Sweden, (1997).
16. P. Zadorecki, P. Mitchell and A. J. Michell, *Polym. Compos.*, Vol. 10, 69, (1989).
17. I. H. Updegraf in *Encyclopedia of Polymer Science and Engineering, 2 ed.*, Mark, Bikales, Overberger and Menges, Eds., John Wiley & Sons (1986).
18. L. Hua, P. Flodin and T. Rönnhult, *Polym. Comp.*, Vol. 8, 203, (1987).
19. L. Hua, P. Zadorecki and P. Flodin, *Polym. Comp.*, Vol. 8, 199, (1987).